

Thermal conductivity of epitaxial graphene nanoribbons on SiC: effect of substrate

Zhi-Xin Guo^{1*}, J. W. Ding¹ and Xin-Gao Gong²

¹*Department of Physics, Xiangtan University, Xiangtan, Hunan 411105, China*

²*Surface Physics Laboratory and Department of Physics, Fudan University, Shanghai 200433, China**

(Dated: September 7, 2018)

We study the effect of SiC substrate on thermal conductivity of epitaxial graphene nanoribbons (GNRs) using the nonequilibrium molecular dynamics method. We show that the substrate has strong interaction with single-layer GNRs during the thermal transport, which largely reduces the thermal conductivity. The thermal conductivity characteristics of suspended GNRs are well preserved in the second GNR layers of bilayer GNR, which has a weak van der Waals interaction with the underlying structures. The out-of-plane phonon mode is found to play a critical role on the thermal conductivity variation of the second GNR layer induced by the underlying structures.

PACS numbers:

Graphene and Graphene nanoribbons (GNRs) are thought to be ideal materials for nanoelectronics due to their outstanding electronic and thermal properties[1–6]. In the production, the graphene nanomaterials can be either prepared by mechanical exfoliation from graphite[7, 8] or by epitaxial growth on SiC substrate[9, 10]. However, the mechanical method is quite delicate and time consuming, which makes it unapplicable in the industry. The epitaxial growth method is nowadays commonly accepted to represent a viable method of controllable growth for the fabrication of high quality graphene wafers[11]. The electronic properties of epitaxial graphene on SiC substrate had been extensively studied[10, 12–14]. It was found the electronic properties of graphene can be well preserved in both the single-layer (SL) graphene on SiC (000 $\bar{1}$) (C-terminated)[10], and the second layer of bilayer (BL) graphene on SiC(0001)(Si-terminated)[12, 13], having great application potential of epitaxial graphene in the nanoelectronics. Since the heat removal is a crucial issue in the nanoelectronic industry, the thermal conduction property of epitaxial graphene and GNRs becomes particularly important to its application in the nanoelectronics.

During the last two years, the thermal conductivity of exfoliated graphene on different substrates (SiO₂, Cu) has been extensively studied, where only weakly coupled graphene-substrate interaction exists[15–19]. Different from the exfoliated graphene case, the epitaxial graphene-substrate interaction is much more complicated, and the geometry can even be distorted by the substrate [12, 20]. Thus the thermal conductivity of epitaxial graphene and GNRs is expected to be very different from the exfoliated ones.

In this work, we use the nonequilibrium molecular dynamics (NEMD)[6, 21–23] method to study the thermal conductivity of epitaxial GNRs on 4H-SiC (000 $\bar{1}$) and (0001) surface. On the (000 $\bar{1}$) surface, both covalently bonded and weakly coupled GNR-substrate interaction

conditions that were observed by the experiments are considered. On the (0001) surface, we consider both the SL and BL GNR-substrate interaction cases. In the BL GNR, we concentrate on the thermal conductivity of the second layer since the first layer is expected to have similar thermal conductivity as the SL GNR. Two typical GNRs, i.e., armchair GNR (AGNR) and zigzag GNR (ZGNR), are considered, and we refer to AGNR/ZGNR with N dimer lines in width as N-AGNR/N-ZGNR for convenient representation[24].

The 4H-SiC substrate is modeled with four alternating Si and C atomic layers. One Si-C layer at the bottom of the sample is fixed. GNRs are placed on top of the SiC substrate, with infinite length along the X direction and finite width along Y direction. The smallest cell of the GNR-SiC system is of 10.12 nm in length (X direction) and 2.15 nm (around 1 nm) for the SiC (GNR) in width (Y direction), containing 2128 SiC atoms and 320 (368) 4-ZGNR (8-AGNR) atoms, respectively.

In the geometry optimization, periodic boundary conditions are applied both along the X and Y directions. We use the Tersoff[25] potential to describe the C-C and C-Si bonded interactions, and the non-bonded van der Waals interaction is described by the Lennard-Jones (LJ) potential[26], which is only nonzero after the Tersoff covalent potential goes to zero. The coupling between the long-range LJ potential and the short-range Tersoff potential is described by a cubic spline function[27].

In the NEMD simulation, we employ the velocity Verlet method to integrate equations of motion with a fixed time step of 1 fs. Fixed boundary condition is applied along the X direction, where the outmost layers of each end of GNR (SiC) are fixed. Next to the boundaries, the adjacent 1 nm-long GNR (SiC) layers are coupled to the Nosé-Hoover[28] thermostats with temperatures 310 and 290 K, respectively. The thermal conductivity of GNRs κ is then calculated from the Fourier law,

$$\kappa = -\frac{J}{\nabla T \cdot S}, \quad (1)$$

where J is the heat flux from the thermostats to the system, which is obtained from the Green-Kubo relation[29,

*Electronic address: zxguo08@gmail.com

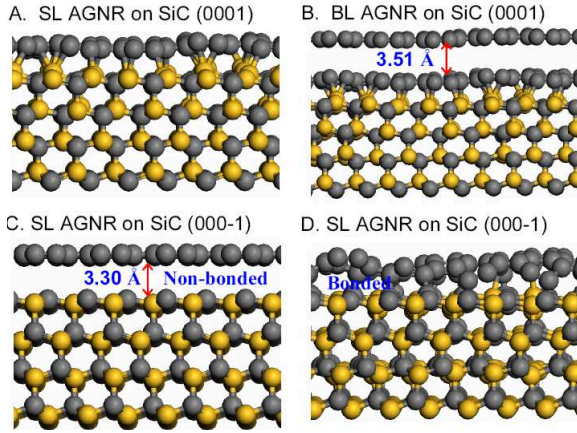


FIG. 1: Optimized structures of 8-AGNR on SiC substrate for 4 cases: A, single-layer GNR on SiC (0001); B, bilayer GNR on SiC (0001); C, single-layer GNR on SiC (000 $\bar{1}$) with weakly coupled interaction; D, single-layer GNR on SiC (000 $\bar{1}$) with covalently bonded interaction. Carbon atoms are represented by gray balls; Si, by yellow balls.

30]. ∇T is the temperature gradient in the length direction, which is defined as $\nabla T = (T_L - T_R)/L$, where T_L , T_R are the temperature of thermostats at the two ends, and L is GNR length. S is the cross-section area. In this work, we choose the interplanar spacing of graphite 3.35 Å as the GNRs' thickness. Moreover, all results given in this paper are obtained by averaging about 5 ns after a sufficient long transient time (5 ns) when a nonequilibrium stationary state is set up.

The following 4 kinds of epitaxial GNRs on SiC are considered: A, SL GNR on SiC (0001); B, BL GNR on SiC(0001); C, SL GNR on SiC (000 $\bar{1}$) with the weakly coupled interaction; D, SL GNR on SiC (000 $\bar{1}$) with the covalently bonded interaction. Before geometry optimization, the initial distance between GNR and SiC surface was set to be 2.3 Å in cases A and B, 3.0 Å in case C, and 2.0 Å in case D. In Fig. 1, we show the optimized structures of 8-AGNR on SiC for the above 4 cases. As one can see, the SL GNRs can either covalently bonded or weakly coupled to the substrate. In the covalently bonded case (case A, D), the formed C-Si (C-C) covalent bond between GNR and substrate has a length around 2.15 (1.60) Å in the middle region, being consistent with the bond length of the graphene-SiC system in previous reports [12, 13, 31]. While, in the edge region the C-Si (C-C) bond length is only about 2.10 (1.50) Å, shorter than the bond length in the middle region, indicating that the edge atoms make the interaction between GNR and substrate stronger than that between graphene and substrate. In the weakly coupled case (case C), the mean distance between GNR and SiC surface is 3.30 Å, similar with the graphene case[32].

In the BL GNR (case B), while, the mean distance between the first and the second layer is 3.51 Å, obviously

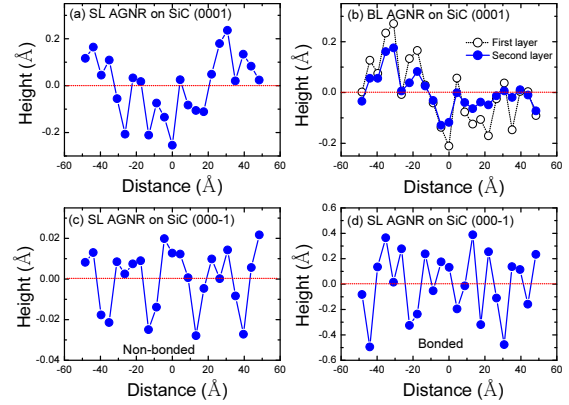


FIG. 2: The height profile of GNRs on SiC along the length direction for cases A (a), B (b), C (c), and D (d).

larger than the interlayer distance of the suspended BL graphene. The larger interlayer distance comes from the larger shear modules of GNRs[33] and the large ripples formed on first GNR layer due to its strong interaction with SiC surface[34]. Compared with the BL graphene, the interlayer force in BL GNR is smaller due to its finite width, while its shear modules is much larger. Thus, unlike the BL graphene, the weak interlayer van der Waals force can't make the second GNR layer follows the large ripples of the first GNR layer, and the second GNR layer still keeps a relatively planar structure. The large interlayer distance appears at the trough of the ripple in first GNR layer.

The corresponding height profile of GNRs on SiC along the length direction is shown in Fig. 2. From the figure, the ripples of GNRs that covalently bonded with SiC are obviously larger than that of GNR weakly coupled with SiC. The smallest and largest ripples appear in case C and D, respectively, both of which are on SiC (000 $\bar{1}$). Moreover, in the BL GNR the ripple of the second GNR layer is obviously smaller than that of first GNR layer (Fig. 2(b)), which corresponds to a larger interlayer distance as discussed above.

Fig. 3 shows the width dependence of thermal conductivity of both AGNRs and ZGNRs on SiC. As shown in the figure, the thermal conductivity of GNRs covalently bonded with SiC is very different from that weakly coupled with SiC. In the covalently bonded case, thermal conductivity of GNRs is very low (below 30 W/mK), and has little variation when the width gets larger than 2 nm. This shows that the strong covalent Si-C/C-C bonds formed between GNR and SiC surface have destroyed the intrinsic thermal conductivity of GNRs. In addition, the thermal conductivity of GNR on SiC (000 $\bar{1}$) (case D) is distinctly smaller than that on the (0001) surface (case A). This is attributed to the larger GNR ripples formed on the (000 $\bar{1}$) surface than that on (0001) surface (Fig. 2), which would induce stronger phonon scattering. Different from the covalently bonded cases, thermal

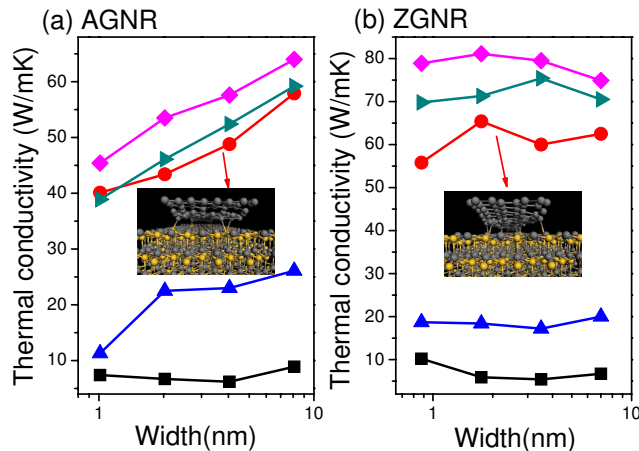


FIG. 3: Width dependence of thermal conductivity of both AGNRs (a) and ZGNRs (b) on SiC in cases A (blue up-triangle), B (cyan right-triangle), C (red circle), and D (black square), with comparison of the suspended GNRs (magenta diamond).

conductivity of GNRs weakly coupled with SiC is much higher (case C). However, we find that some C-Si covalent bonds are newly formed between the edge of SL GNR and SiC(000 $\bar{1}$) surface during the NEMD simulation (inset of Fig. 3), which is attributed to the large atomic amplitude of GNR in the direction perpendicular to the SiC surface when the system is thermostated to 300 K. The covalent bonds would induce additional edge localized phonon scattering on the GNR, and thus reduce the thermal conductivity. Since the number of newly formed covalent bonds is proportional to the length of GNR, compared with that of the suspended GNR, we expect the thermal conductivity will be largely reduced when the GNR length gets to μm -scale (experimental length).

From Fig. 3, it is definite that, the thermal conductivity of the second GNR layer in a BL GNR (case B) is most close to that of the suspended GNR. Also, the width-dependence of thermal conductivity is very similar to each other: With the width increasing, the thermal conductivity of AGNR monotonously increases, while the thermal conductivity of ZGNR increases first and then decreases[6]. This implies the weak van der Waals interaction from underlying structures (both the first GNR layer and SiC substrate) does not break the intrinsic thermal conductivity of the second GNR layer.

In Fig. 4 we show the length dependence of thermal conductivity of the second GNR layers of BL GNR with comparison of the suspended GNRs. Similar with that of the suspended GNRs and carbon nanotubes[6, 35], the thermal conductivity of the second 8-AGNR (4-ZGNR) layer monotonously increases with the length increasing and follows a power law of $\kappa \sim L^\beta$, with $\beta=0.38$ (0.49). The value of β is very close to that of the suspended GNR ($\beta=0.32$ (0.50)), showing that the ballistic and 1D thermal transport characters[35–37] are well preserved in

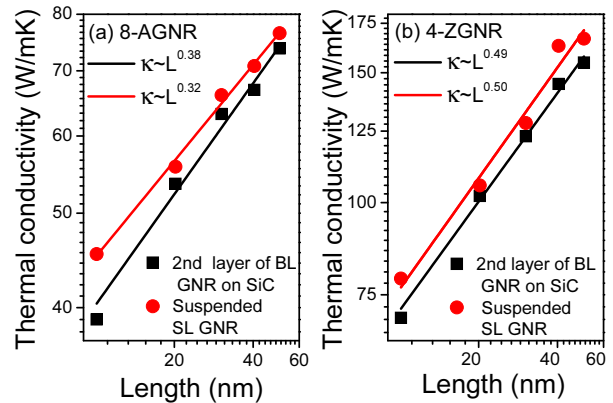


FIG. 4: Thermal conductivity κ vs the length L in log-log scale for the second 8-AGNR (a), 4-ZGNR (b) layers in BL GNR, with comparison of the suspended GNRs. In both cases, $\kappa \sim L^\beta$, with β being close to that of the suspended GNRs.

TABLE I: Thermal conductivity κ of 8-ZGNRs with/without the out-of-plane vibrational constraint. The GNR length is kept at 10 nm.

GNR type	Constraint	κ (W/mK)
Suspended SL GNR	Free	81.1
Suspended SL GNR	Constraint	77.7
2nd layer of BL GNR	Free	71.3
2nd layer of BL GNR	Constraint	79.1

the second GNR layer.

To further explore the substrate effect on thermal conductivity of the second GNR layer of BL GNR on SiC, we freeze the out-of-plane atomic vibration of the second GNR layer and recalculate the thermal conductivity with comparison of the suspended SL GNR. For simplicity, here we only present the calculated thermal conductivity of ZGNRs, similar result is also obtained for AGNRs. As shown in Table 1, freezing the out-of-plane atomic vibration decreases the thermal conductivity of the suspended SL GNR, while it considerably increases the thermal conductivity of the second GNR layer of BL GNR.

This illustrates two facts. One is that the out-of-plane phonon mode in suspended SL GNR has a positive contribution to the thermal transport, although it is not dominating. The other is that the thermal conductivity reduction of the second GNR layer of BL GNR mainly comes from the coupling between its out-of-plane phonon mode and the phonon modes of the underlying structures (including phonon modes of both first GNR layer[38] and SiC surface). It should be mentioned that, the thermal conductivity of the second GNR layer (79.1 W/mK) in BL GNR is even higher than that of the suspended SL GNR (77.7 W/mK) when the out-of-plane atomic vibration is frozen. This interesting phenomenon indicates an increment of thermal conductivity can be re-

alized through the substrate coupling without the out-of-plane phonon. Recently, through a coupled atomic chain model, we have clarified that there exists a competitive mechanism on thermal conductivity in a coupling system: the phonon resonance effect that decreases thermal conductivity and phonon-band-up-shift effect that increases thermal conductivity[23]. In this case, the phonon resonance effect mainly comes from the coupling between out-of-plane phonon mode of the second GNR layer and the phonon modes of the first GNR layer and SiC substrate. When the out-of-plane atomic vibration is frozen, the phonon resonance effect would be largely reduced, and the phonon-band-up-shift effect become dominated. Thus the thermal conductivity can be increased by the coupling. The results further confirm the existence of two competitive effects between the thermal conductive material and substrate.

In summary, we have investigated the thermal conductivity of epitaxial SL and BL GNRs on SiC substrate using the NEMD method. For the SL GNR, both covalently bonded and weakly coupled GNR-substrate interaction conditions that were observed by experiments are considered. The thermal conductivity of SL GNRs

in the covalently bonded condition is particularly low, while it is much higher in the weakly coupled condition. However, there appear some C-Si covalent bonds between the edge of SL GNR and SiC surface in the weakly coupled condition during the thermal transport, which induces additional edge localized phonon scattering and is expected to largely reduce the thermal conductivity when the GNR length gets to μm -scale. The second GNR layer of BL GNRs is found to have the highest thermal conductivity among all the epitaxial GNRs, and keeps much the same thermal conductivity characteristics as the suspended GNR. We find that the out-of-plane phonon mode of the second GNR layer plays a critical role on the thermal conductivity variation induced by the underlying structures. The existence of two competitive effects between thermal conductive material and substrate is further confirmed. We expect the present study can be helpful to the forthcoming applications of epitaxial graphene nanomaterials in the nanoelectronics.

This work was supported by the Start-up funds (No. 10QDZ11), Scientific Research Fund (10XZX05) of Xiangan University, and PCSIRT (IRT1080).

-
- [1] A. K. Geim, *Science* 324, 1530 (2009).
- [2] A. H. Castro Neto, F. Guinea, N. M. R. Peres, K. S. Novoselov, and A. K. Geim, *Rev. Mod. Phys.* 81, 109 (2009).
- [3] A. A. Balandin, S. Ghosh, W. Bao, I. Calizo, D. Teweldebrhan, F. Miao, and C. N. Lau, *Nano Lett.* 8, 902 (2008).
- [4] A. A. Balandin, *Nature Mater.* 10, 569 (2011).
- [5] J. Hu, X. Ruan, and Y. P. Chen, *Nano Lett.* 9, 2730 (2009).
- [6] Z. X. Guo, D. Zhang, and X. G. Gong, *Appl. Phys. Lett.* 95, 163103 (2009).
- [7] K. S. Novoselov, A. K. Geim, S. V. Morozov, D. Jiang, M. I. Katsnelson, I. V. Grigorieva, S. V. Dubonos, and A. A. Firsov, *Nature* 438, 197 (2005).
- [8] Y. Zhang, Y. W. Tan, H. L. Stormer, and P. Kim, *Nature* 438, 201 (2005).
- [9] W. A. de Heer, C. Berger, X. S. Wu, P. N. First, E. H. Conrad, X. B. Li, T. B. Li, M. Sprinkle, J. Hass, M. L. Sadowski, M. Potemski, and G. Martinez, *Solid State Commun.* 143, 92 (2007).
- [10] K. V. Emtsev, F. Speck, T. Seyller, L. Ley, and J. D. Riley, *Phys. Rev. B* 77, 155303 (2008).
- [11] C. Dimitrakopoulos, Y. M. Lin, A. Grill, D. B. Farmer, M. Freitag, Y. Sun, S. J. Han, Z. Chen, K. A. Jenkins, Y. Zhu, Z. Liu, T. J. McArdle, J. A. Ott, R. Wisnieff, and P. Avouris, *J. Vac. Sci. Technol. B* 28, 985 (2010).
- [12] A. Mattausch, and O. Pankratov, *Phys. Rev. Lett.* 99, 076802 (2007).
- [13] F. Varchon, R. Feng, J. Hass, X. Li, B. NgocNguyen, C. Naud, P. Mallet, J. Y. Veuillein, C. Berger, E. H. Conrad, and L. Magaud, *Phys. Rev. Lett.* 99, 126805 (2007).
- [14] S. Kim, J. Ihm, H. J. Choi, and Y. W. Son, *Phys. Rev. Lett.* 100, 176802 (2008).
- [15] J. H. Seol, I. Jo, A. L. Moore, L. Lindsay, Z. H. Aitken, M. T. Pettes, X. Li, Z. Yao, R. Huang, D. A. Broido, N. Mingo, R. S. Ruoff, and L. Shi, *Science* 328, 213 (2010).
- [16] W. Jang, Z. Chen, W. Bao, C. N. Lau, and C. Dames, *Nano Lett.* 10, 3909 (2010).
- [17] Y. K. Koh, M. H. Bae, D. G. Cahill, and E. Pop, *Nano Lett.* 10, 4363 (2010).
- [18] Z. Wang, R. Xie, C. T. Bui, D. Liu, X. Ni, B. Li, and T. L. J. Thong, *Nano Lett.* 11, 113 (2011).
- [19] Z. Y. Ong, and E. Pop, *Phys. Rev. B* 84, 075471 (2011).
- [20] V. Sorkin, and Y. W. Zhang, *Phys. Rev. B* 81, 085435 (2010).
- [21] Z. X. Guo, D. Zhang, Y. T. Zhai, and X. G. Gong, *Nanotechnology* 21, 285706 (2010).
- [22] Z. X. Guo, and X. G. Gong, *Front. Phys.* 4, 389 (2009).
- [23] Z. X. Guo, D. Zhang, and X. G. Gong, *Phys. Rev. B* 84, 075470 (2011).
- [24] Y. W. Son, M. L. Cohen, and S. G. Louie, *Phys. Rev. Lett.* 97, 216803 (2006).
- [25] J. Tersoff, *Phys. Rev. B* 39, 5566 (1989).
- [26] L. A. Girifalco, M. Hodak, and R. S. Lee, *Phys. Rev. B* 62, 13104 (2000).
- [27] Z. Mao, A. Garg, and S. B. Sinnott, *Nanotechnology* 10, 273 (1999).
- [28] S. Nosé, *J. Chem. Phys.* 81, 511 (1984); W. G. Hoover, *Phys. Rev. A* 31, 1695 (1985).
- [29] P. K. Schelling, S. R. Phillpot, and P. Keblinski *Phys. Rev. B* 65, 144306 (2002).
- [30] N. Yang, G. Zhang, and B. Li, *Nano Lett.* 8, 276 (2008).
- [31] Y. Qi, S. H. Rhim, G. F. Sun, M. Weinert, and L. Li, *Phys. Rev. Lett.* 105, 085502 (2010).
- [32] F. Hiebel, P. Mallet, J. Y. Veuillein, and L. Magaud, *Phys. Rev. B* 83, 075438 (2011).
- [33] R. Faccio, P. A. Denis, H. Pardo, C. Goyenola, and Á. W. Mombrú, *J. Phys.: Condens. Matter* 21, 285304 (2009).

- [34] F. Varchon, P. Mallet, J. Y. Veuille, and L. Magaud, *Phys. Rev. B* 77, 235412 (2008).
- [35] S. Maruyama, *Physica B* 323, 193 (2002).
- [36] E. Enrique, J. Lu, and B. I. Yakobson, *Nano Lett.* 10, 1652 (2010).
- [37] G. Zhang, and B. Li, *J. Chem. Phys.* 123, 114714 (2005).
- [38] H. Y. Cao, Z. X. Guo, H. J. Xiang, and X. G. Gong, *Phys. Lett. A* 376, 525 (2012).